

# Durability and physical characterization of anti-fogging solution for 3D-printed clear masks and face shields

Succhay Gadhar<sup>Equal first author, 1</sup>, Shaina Chechang<sup>Equal first author, 1</sup>, Philip Sales<sup>1</sup>, Praveen Arany<sup>Corresp. 1</sup>

<sup>1</sup> Oral Biology, Biomedical Engineering, and Surgery, University at Buffalo, Buffalo, NY, USA

Corresponding Author: Praveen Arany  
Email address: praveenarany@gmail.com

**Background.** The COVID-19 pandemic brought forth the crucial roles of personal protective equipment (PPE) such as face masks and shields. Additive manufacturing with 3D printing enabled customization and generation of transparent PPEs. However, these devices were prone to condensation from normal breathing. This study was motivated to seek a safe, non-toxic, and durable anti-fogging solution. **Methods.** We used additive 3D printing to generate the testing apparatus for contact angle, sliding angle, and surface contact testing. We examined several formulations of carnauba wax to beeswax in different solvents and spray-coated them on PETG transparent sheets for testing contact and sliding angle, and transmittance. Further, the integrity of this surface following several disinfection methods such as soap, Isopropyl Alcohol, or water alone with gauze, paper towels, and microfiber, along with disinfectant wipes, was assessed. **Results.** The results indicate a 1 : 2 ratio of carnauba to beeswax in Acetone optimally generated a highly hydrophobic surface (contact angle  $150.3 \pm 2.1^\circ$  and sliding angle  $13.7 \pm 2.1^\circ$ ) with maximal transmittance. The use of soap for disinfection resulted in the complete removal of the anti-fogging coating, while Isopropyl Alcohol and gauze optimally maintained the integrity of the coated surface. Finally, the contact surface testing apparatus generated a light touch ( $5000 \text{ N/m}^2$ ) that demonstrated good integrity of the antifogging surface. **Conclusions:** This study demonstrates that a simple natural wax hydrophobic formulation can serve as a safe, non-toxic, and sustainable anti-fogging coating for clear PPEs compared to several commercial solutions.

1     **Durability and Physical Characterization of Anti-Fogging**  
2     **Solution for 3D-Printed Clear Masks and Face Shields**

3             Succhay Gadhar<sup>1,\*</sup>, Shaina Chechang<sup>1,\*</sup>, Philip Sales<sup>1</sup>, Praveen R. Arany<sup>1,\$</sup>

4             <sup>1</sup> Oral Biology, Biomedical Engineering and Surgery, University at Buffalo, NY, USA

5     \* *Equal contributions*

6

7     <sup>\$</sup>**Address correspondence to:**

8     Praveen R. Arany B.D.S., M.D.S., M.M.Sc., Ph.D.

9     3435 Main Street, BRB 553,

10    Buffalo, NY 14214.

11    E-mail: [prarany@buffalo.edu](mailto:prarany@buffalo.edu)

12    Phone: 716-829-3479

13

14

15    **Keywords:** Face shields, Masks, Anti-fogging

16

17

18

19 **ABSTRACT**

20 **Background.** The COVID-19 pandemic brought forth the crucial roles of personal protective  
21 equipment (PPE) such as face masks and shields. Additive manufacturing with 3D printing enabled  
22 customization and generation of transparent PPEs. However, these devices were prone to  
23 condensation from normal breathing. This study was motivated to seek a safe, non-toxic, and  
24 durable anti-fogging solution.

25 **Methods.** We used additive 3D printing to generate the testing apparatus for contact angle, sliding  
26 angle, and surface contact testing. We examined several formulations of carnauba wax to beeswax  
27 in different solvents and spray-coated them on PETG transparent sheets for testing contact and  
28 sliding angle, and transmittance. Further, the integrity of this surface following several disinfection  
29 methods such as soap, Isopropyl Alcohol, or water alone with gauze, paper towels, and microfiber,  
30 along with disinfectant wipes, was assessed.

31 **Results.** The results indicate a 1 : 2 ratio of carnauba to beeswax in Acetone optimally generated  
32 a highly hydrophobic surface (contact angle  $150.3 \pm 2.1^\circ$  and sliding angle  $13.7 \pm 2.1^\circ$ ) with  
33 maximal transmittance. The use of soap for disinfection resulted in the complete removal of the  
34 anti-fogging coating, while Isopropyl Alcohol and gauze optimally maintained the integrity of the  
35 coated surface. Finally, the contact surface testing apparatus generated a light touch ( $5000 \text{ N/m}^2$ )  
36 that demonstrated good integrity of the antifogging surface.

37 **Conclusions:** This study demonstrates that a simple natural wax hydrophobic formulation can  
38 serve as a safe, non-toxic, and sustainable anti-fogging coating for clear PPEs compared to several  
39 commercial solutions.

40

41

42

43

44

45

## 46 INTRODUCTION

47 The COVID-19 pandemic has had a significant toll on the public health, biomedical, and  
48 financial aspects that have significantly changed society.(1,2) Among various healthcare services,  
49 the presence of SARS-CoV in the nasal and upper respiratory tract presented significant challenges  
50 for dentists and anesthetists. Clinical dentistry presented a significant challenge due to the  
51 proximity and inherent aerosol-generating procedures.(3-5) The use of personal protection  
52 equipment (PPE) such as face masks and face shields was integral in reducing the spread of  
53 infections among the general population. (6) While dentistry routinely utilizes face masks, double  
54 masking, and the highly protective N95, the shielding nature and the lack of face-to face exposure  
55 further compounded the pandemic fear and anxiety in patients naturally apprehensive about their  
56 dental visits. (7-9) Another major limitation of these masks is that they hinder effective  
57 communication due to the lack of non-verbal cues such as facial expressions and lips movements.  
58 (10-12) This is particularly challenging in patients with differently-abled hearing due to increased  
59 signal-to-noise from the ambient noise in dental operatories. (13-16) The use of transparent masks  
60 and face shields has been demonstrated to improve these limitations. (17)

61 Another major challenge during the early phase of the pandemic was the significant  
62 disruption of the PPE supply chain requiring local innovations where additive manufacturing using  
63 3D printing came to the forefront. (18-21) The ability to generate required quantities based on need  
64 and additional customization for individual applications were significant advantages of this  
65 approach. (22) Building on this, in collaboration with e-NABLE, a 3D printing community,  
66 students at the University at Buffalo School of Dental Medicine generated transparent PPEs using  
67 3D printing and vacuum casting. Among them, several custom designs were specifically generated  
68 to accommodate commercially available dental loupes that are made available freely online.(23)  
69 These clear masks and face shields were well accepted and generated much enthusiasm among  
70 clinical users. Besides dentistry, another group of clinicians that notably adopted these clear PPEs  
71 were the local speech and hearing-impaired clinics. However, an immediate limitation of this  
72 approach reported by users was the fogging due to the moisture from regular breathing. This  
73 essentially negated the advantage of the transparent nature of these masks and face shields and  
74 presented additional hindrance of needing repetitive wipe-downs.

75 The commercially available anti-fogging solutions used for eyeglasses and car exteriors  
76 contain polydimethylsiloxane and silica nanoparticles.(24) The long-term use of these solutions  
77 was considered unsuitable due to their potential for skin irritation, and potential inhalation or  
78 ingestion. Hence, we sought to identify a non-toxic, antifogging coating for the transparent masks  
79 and face shields for long-term use. To design such a solution, specific design criteria needed to be  
80 met. The surface of a water droplet is attracted to the bulk of the droplet due to cohesion which  
81 results in their beading. The shape that a drop takes on a given surface depends on the surface  
82 tension of the fluid and the physical characteristics of the surface. A surface-fluid interface is the  
83 contact angle that measures the wettability of a surface. Contact angles can vary from hydrophilic  
84 (less than or equal to  $30^\circ$ ) to hydrophobic (greater than or equal to  $120^\circ$ ), where the higher the  
85 contact angle, the lower its wettability. (25) Another measure of the extent of moisture retention  
86 on a surface is the sliding angle which is measured by tilting the surface with the solution bead to  
87 determine the angle at which it rolls off. The more hydrophobic the surface, the higher the angle  
88 of loss of fluid droplets.(26) Another key design aspect of the anti-fogging solution would be its  
89 resistance to wear due to repeated skin surface contact during mask use. The ideal solution would  
90 offer a thin, durable coating for daily use that would not need repetitive applications while  
91 maintaining maximal transparency.

92 Natural products offer attractive non-toxic coatings. Prior studies have examined the  
93 combination of cinnamon and nutmeg that produces high hydrophobicity.(27) Although both are  
94 natural products, this paper utilized a organosilane-based alkyl and perfluorinated synthetic  
95 chemical coatings that raised some toxicity concerns due to high cuprous oxide content. We drew  
96 inspiration from the naturally occurring, extremely hydrophobic lotus leaves. These leaves expel  
97 water easily due to their micro-structural features, termed papillae, that exude epicuticular waxes,  
98 cutin.(28,29) Alternatively, Carnauba and beeswax have also high hydrophobicity that are  
99 routinely used in the food service industry.(30) With their high hydrophobicity, these solutions on  
100 food containers prevent waste by ensuring minimal food retention. However, there was a lack of  
101 clarity in the concentrations used in these prior formulations and the resulting hydrophobicity. The  
102 present study examined the different formulations of these two waxes together and evaluated the  
103 contact angle, sliding angle, and transmittance. The optimized formulation was subjected to  
104 durability testing with manual disinfectant procedures and long-term contact-wear testing.

## 105 MATERIALS AND METHODS

### 106 Formulation of anti-fogging solutions

107 Hydrophobic wax coatings were generated in acetone or methanol as solvents using  
108 ultrasonication. Different ratios of carnauba wax to beeswax (both Sigma Aldrich, St. Louis, MO)  
109 were employed namely 0.4375 g: 0.4375 g (1:1), 0.35 g: 0.525 g (1:1.5), 0.33 g: 0.66 g (1:2), 0.417  
110 g: 0.834 g (1:2HC) were melted in a 50 ml plastic tube (Corning, Thermofisher Waltham, MA) in  
111 a water bath. After the waxes had melted, 25 milliliters of either acetone or methanol (both Sigma  
112 Aldrich, St. Louis, MO) were added, and the solution was emulsified immediately using a probe  
113 ultrasonication (Q2000, QSonica, Newtown CT) at 90% amplitude for 3 minutes and transferred  
114 into a 50 ml glass spray bottle.

### 115 Contact and Sliding Angle testing

116 Solutions were sprayed onto a 2 x 2-inch sheet of PETG at roughly a distance of 5 inches, spraying  
117 10 times. After drying, the sheets of PETG were tested for contact angle, sliding angle, and  
118 transmission. A custom contact and sliding angle device were generated based on commercially  
119 available models using online CAD software (Onshape, PTC, Rockwell Automation, Boston MA).  
120 The devices were printed using Polylactic acid (PLA) filament (Overture, Overture 3D  
121 Technologies, Texas) on a i3 Prusa 3D printer (Prusa Research, Prague Czech Republic) (**Figs. 1**  
122 **A - C**). The device included a slot for to hold a mobile phone to take digital pictures of the droplet.  
123 After fixing the plastic surface to the platform, droplets of water were generated with a 3 ml syringe  
124 and 14-gauge needle (to mimic humidity post-condensation on clear PPEs) and digital image were  
125 captured for analysis (**Fig. 1 D**). The digital images were analyzed using the NIH ImageJ (ver.  
126 1.53n) software. The sliding angle set up included a protractor to assess the angle at which the  
127 droplet slides off. The platform was tilted slowly until the water droplet slid off, and the angle was  
128 documented (**Fig. 1 E**). All studies were performed in performed in triplicate and repeated at least  
129 twice.

### 130 Transmittance analysis

131 The laser apparatus consisted of a 650 nm diode laser (Weber Medical, Beverungen, Germany) at  
132 10 mW/cm<sup>2</sup>, and a sensor with power meter (both Thor Labs, Newton NJ) (**Fig. 1F**). The sheets  
133 of PETG were placed on top of the power sensor, and transmission was assessed.

**134 Optical clarity analysis**

135 A sticker was placed on a bench and the sheets of PETG were placed over it. Digital pictures were  
136 taken with a mobile phone camera. The coated sheets of PETG were compared with the uncoated  
137 control and the visual clarity of the coatings was assessed.

**138 Routine manual disinfection testing**

139 The PETG coated surfaces were subjected to different solutions such as soap solution (10% v/v,  
140 Dawn, Procter & Gamble, Cincinnati OH), Isopropyl alcohol (70%, Sigma Aldrich, St. Louis MO),  
141 and water alone using paper towels (Uline, Milton ON), gauge (Henry Schein, New York, NY) or  
142 microfibers (Magic Fiber, Miami FL). These disinfectants were applied ten times in a uniform,  
143 lateral motion with manual pressure by a single operator. Disinfection wipes (Metrex, Orange CA)  
144 were used in another group.

**145 Coating Durability following contact wear testing**

146 To simulate accelerated contact wear testing, a custom apparatus was designed to mimic skin  
147 contact. Using the CAD software (Onshape, PTC, Rockwell Automation, Boston MA), a rotating  
148 platform with spring-loaded bases was designed to apply suitable skin contact forces. (31-33) The  
149 device was 3D printed with PLA filament (Overture, Overture 3D Technologies, Texas) on a i3  
150 Prusa 3D printer (Prusa Research, Prague Czech Republic). The wheel was connected to a DC  
151 Motor (Greartisan, Shenzhen Hotec, China) via a speed controller and a 9V battery which allowed  
152 the motor to function up to 1000 RPMs. After the coated samples were mounted on the platforms,  
153 the apparatus was positioned to allow the platforms to extend and retract using centrifugal force  
154 while spinning, hitting a skin-equivalent surface (rough side of oil-treated leather) to simulate  
155 contact. To simulate multiple skin contacts, the device was operated for 5 minutes, allowing each  
156 platform to contact the wall about 5000 times for each sample to simulate 4 weeks of routine wear.  
157 The contact force applied by the rotational, spring-loaded platform was measured with a digital  
158 force probe (Baoshishan, China). Following the contact wear testing, samples were assessed for  
159 changes in contact angle, sliding angle, transmittance and examined with topological analysis.

160

161

## 162 **Topological analysis**

163 Scanning electron microscopy (SEM) analysis was performed to determine the topology and the  
164 depth of the coating on the plastic sheet samples prior to and following wear testing. Samples were  
165 sputter-coated (Cressington 108, Ted Pella Inc, Redding CA) with carbon for 120 seconds and  
166 examined using SEM (Hitachi, S-4700, Japan) with a voltage of 2.0 kV at about  $14.5 \pm 0.4$  mm  
167 using secondary electron mode.

## 168 **Statistical Analysis**

169 Data was organized in Excel (Microsoft, Seattle WA) and presented as Means with standard  
170 deviations. Data was subjected to a Student's T test or two-way analysis of variance (ANOVA)  
171 among different treatments with Bonferroni's correction for multiple comparisons where  
172 appropriate. A  $p < 0.05$  was considered statistically significant.

## 173 **RESULTS**

### 174 **Formulation and Characterization of Anti-Fogging solutions**

175 We first examined different ratios of carnauba and beeswax in two solvents namely  
176 Acetone and Ethanol to generate a homogenous solution (**Fig. 2A**). The contact angles of the  
177 acetone-based solutions were higher than their methanol counterparts (**Figs. 2B** and **2C**). The  
178 coating with the highest contact angle was the 1: 2 ratio in acetone solution with a mean contact  
179 angle of  $150.3 \pm 2.1$  °. This categorizes this surface coating as highly hydrophobic compared to  
180 the other coatings and was significantly ( $p < 0.05$ ) more hydrophobic than the uncoated plastic  
181 surface. We also examined the higher concentrations (HC) at 1 : 2 ratio to inquire if the density  
182 and hence, eventual coating concentration would affect these properties, but did not observe any  
183 further significantly improved characteristics. As expected the sliding angle for this coating was  
184 the lowest at  $13.7 \pm 2.1$ ° which was significantly ( $p < 0.05$ ) lower than the uncoated plastic surface  
185 (**Figs. 2D** and **2E**). The transmittance of these formulation appears to vary with the concentration  
186 of the beeswax component as lower amounts resulted in higher transmittance (**Figs. 2F** and **2G**).  
187 The optical clarity was also assessed through the observation of the sticker through the coated  
188 slides. The optical clarity decreased as the concentrations of the solutes increased as was expected.  
189 The methanol-based formulations had a comparable degree of transmittance (0.41 to 0.33) than  
190 the acetone (0.3 to 0.26) counterparts compared to control (uncoated  $0.43 \pm 0.02$ ). Based on these

191 results, we decided to pursue the 1:2 carnauba to bee wax in acetone formulation for subsequent  
192 studies.

### 193 **Effect of routine disinfection procedures on durability of antifogging solution**

194 The use of disinfectants is a necessary part of routine plastic mask and face shield use due  
195 to the prominent aerosol generating dental procedures. (34-36) Next, we examined routine  
196 disinfectant procedures employed in the dental office namely, soap, water, and 70% Isopropyl  
197 Alcohol with paper towels, gauze, or microfiber, and disinfectant wipes. We noted a significant ( $p$   
198  $< 0.05$ ) reduction in the contact angle after all disinfection methods (**Fig. 3A**). Among all these  
199 methods, Isopropyl Alcohol with gauze reduced the contact angle the least ( $144.3 \pm 1.6^\circ$ ) while  
200 soap made the surface most hydrophilic (wettable), removing the coating most effectively.  
201 Concurrently, the sliding angle analysis showed a similar trend, increasing overall with all, but the  
202 soap group, disinfection methods (**Fig. 3B**). The Isopropyl alcohol group showed the least change  
203 and no statistically significant difference was noted when a paper towel was used. Interestingly,  
204 the transmittance appeared to vary after individual disinfectant methods with some showing  
205 increases while other showing significant decreases (**Fig. 3C**). The method of disinfection that  
206 showed most increase in light transmission were the sterilizing wipes by themselves. The lowest  
207 transmission was observed with Isopropyl Alcohol and soap with paper towels. Together, these  
208 results suggest that using Isopropyl Alcohol with gauze is optimal for disinfection as it minimally  
209 affects antifogging coating properties such as contact and sliding angle and transmission after  
210 repeated use.

### 211 **Antifogging coating stability after contact wear testing**

212 Finally, we investigated the durability of the anti-fogging solutions as they would be  
213 subjected to rigorous daily wear and tear during PPE use. We first created a simple rig to simulate  
214 skin contact based on a 3D printed apparatus (**Fig. 4A and B**). The rig was designed as a rotating  
215 platform that would result in a repetitive contact of the coated device with a stationary leather  
216 surface. The pressure exerted by facemask on the nose bridge and chin contact has been assessed  
217 to be 45 to 91 mm of Hg (6000-12,000 N/m<sup>2</sup>) (**Fig. 4C**). (31-33) The constant skin contact force  
218 in our device was assessed to be 5000 N/m<sup>2</sup> that could be approximated to a repeated light skin  
219 contact.

220 Following the simulated wear, the contact and sliding angle as well as transmittance was  
221 assessed. We observed a significant reduction in contact angle ( $133.3 \pm 1.5^\circ$ ) and concomitant  
222 increase in the sliding angle ( $23.7 \pm 1.5^\circ$ ) compared to the uncoated control surfaces. While  
223 transmittance was not significantly different before and after wear simulation, there was a trend  
224 towards reduced transmission. Topological analysis noted the wear simulation resulted in  
225 significant accretions and scratches that likely contribute to the reduced light transmission  
226 observed. These results indicate that due to reduction in coating characteristics by about 50% over  
227 the simulated 4-week wear period, the coating will likely need to be replaced as often as every  
228 other week to maintain optimal functions.

229

## 230 DISCUSSION

231 The COVID pandemic presented new challenges to healthcare with an urgent need for  
232 innovations in disinfection approaches. The use of PPE was central in the attempts to mitigate the  
233 spread of infection and a major part of the solution to mitigate the health crisis. The use of these  
234 barriers continues to have an impact on both the psychological, and medical well-being of both the  
235 patients and the healthcare professionals themselves.(37) The initial response to the pandemic  
236 brought manufacturing and supply chain disruptions resulting in additive 3D printing enthusiasts  
237 to offer custom, local solutions. Our team at the University at Buffalo focused on the transparent  
238 PPE designs and dental loop attachments (**Fig. 5**). The condensation from breathing obscured the  
239 functions of the clear PPEs that presented a major impasse to their use. This work was specifically  
240 motivated to address this deterrent to routine clear PPE use.

241 We tested polyethylene terephthalate glycol (PETG). PETG is a commonly-used  
242 thermoplastic with impact resistance, durability, ductility, chemical resistance properties well-  
243 suited to this application. To generate an anti-fogging solution for our clear face shields and masks,  
244 a major design challenge was the close proximity to nose and mouth.(38,39) We chose to pursue  
245 natural waxes as the main ingredient as they provided a natural, non-toxic solution that has a well-  
246 established track record of biological safety. (40) The other major component constituent was a  
247 polar solvent to enhance miscibility and dispersion of these waxes. We chose to examine Acetone  
248 and Ethanol in our formulation. The acetone formulation was superior in generating the most  
249 hydrophobic product after spray coating. Our initial efforts at dissolving the waxes in Acetone

250 (boiling point of 55.5°C) by heating alone resulted in evaporation and non-uniform dissolution.  
251 Hence, we chose to disperse the waxes via ultrasonication. Among the various formulations, the  
252 most hydrophobic surface was generated by the 1 : 2 ratio (contact angle  $150.3 \pm 2.1^\circ$ ) though the  
253 other formulations were also strongly hydrophobic (contact angles 121 to 135°). We also examined  
254 Methanol (boiling point of 148.5 °F) in the same volume that, in contrast, generated hydrophilic  
255 surface coatings with all formulations (contact angles 34 to 82 °), but most prominently with the 1  
256 : 2 at the higher concentration (contact angle  $80.7 \pm 2.1^\circ$ ). Increasing the concentration in the  
257 Methanol formulation (1 : 2 HC) appeared to impact the physical characteristics more than the  
258 Acetone (1 : 2 HC) formulation that could be attributed to differential dissolution of the waxes and  
259 subsequent homogeneity of the coating film. Among the two solvents examined, Methanol did not  
260 enable a suitable anti-fogging formulation and hence, the 1: 2 formulation in Acetone was chosen  
261 as an optimal anti-fogging solution. This may have been due to the fact that methanol has a higher  
262 polarity than acetone that facilitates improved dispersibility of the non-polar wax compounds.

263         The use of surface disinfectants is an integral part of maintaining and reusing PPEs. This  
264 is a sustainable and cost-effective practice that is routinely employed. A key design requirement  
265 of the anti-fogging solution is durability with these disinfectant approaches. We observed that the  
266 soap solution group consistently demonstrated complete removal of the anti-fogging solution.  
267 While this desirable as a disinfectant approach to remove all potentially hazardous aerosols on  
268 these PPEs, its amphiphilic nature allowing it to form micelles with the wax components of the  
269 anti-fogging solution would deem it unsuitable. The removal of the anti-fogging solution with  
270 these approaches could be attributed to the surfactant nature that interferes with the surface tension  
271 of the water droplets. Another possibility is that the lipid-to-lipid interaction of the soap and the  
272 waxes may inactivate the hydrophobic nature of the coating. The superior solubilizing ability of  
273 isopropyl alcohol that may further smoothen the coating, reduce surface tension further or alter  
274 drying times are areas of future investigations.

275         To investigate the durability of the anti-fogging coating, we generated a custom rig for  
276 accelerated surface contact testing. The major design principle for this device was to generate a  
277 PPE skin contact force. The reported PPE skin contact force to create a tight seal on the nose and  
278 chin has been reported as 45 to 91 mm of Hg (6000-12,000 N/m<sup>2</sup>). (31-33) The force generated by  
279 our rig was lower at 5000 N/m<sup>2</sup> and was intended to approximate light skin contact force in non-

280 fastened areas. This reflects routine surface contact during routine use of the PPEs. The  
281 hydrophobicity of the anti-fogging surfaces was relatively well maintained (contact angle  $133.3 \pm$   
282  $1.5^\circ$  and sliding angle  $23.7 \pm 1.5^\circ$ ). However, the durability testing noted a reduction in the  
283 transmittance of the masks that could be attributed the wear from the contact forces. As evident in  
284 the ultrastructural analysis, the PETG surface appears to have several accretions and disruption of  
285 the uniform coated surfaces. Given these PPEs are disposable and have a limited time of use, this  
286 may not significantly impact the PPE performance. In fact, this lack of clarity from routine use  
287 may be a good marker for replacement with a simple optical interferometry device.

288 This study has a few limitations. First, the biological performance of this anti-fogging  
289 solution could be examined using *in vitro* (reconstructed human epidermis), and *in vivo* skin  
290 contact testing in animals and human studies. (41-47) While this could be considered routine  
291 diligence, it is prudent to emphasize both the waxes and PETG are generally regarded as safe (FDA  
292 GRAS) and are used in current product (e.g; lip balm) formulations routinely. The solvents are  
293 readily eliminated by mild heating ( $40^\circ\text{C}$  overnight). Second, applying a hydrophobic solution on  
294 the PETG clear surface may, counter to its primary objective, worsen the visibility due to the  
295 moisture coalescing into larger water beads. It is conceivable that the increasing size of these water  
296 beads may eventually reach a critical mass and cause them to slide off. This phenomenon is  
297 observed on hydrophobic surfaces like lotus leaves and commercial car wax coatings. Hence, a  
298 replaceable absorbent liner and a mild, mechanical vibration module to promote water droplet  
299 beading and run-off could be attractive future design iteration in these clear PPEs. Third, a major  
300 shortcoming of using such an anti-fogging spray is its temporary nature and the need for  
301 continuous replacement throughout the lifetime of the clear PPE. Thus, a potential future  
302 possibility is to pursue nanopatterning, simulating the lotus leaf papillae for a more biocompatible,  
303 permanent anti-fogging solution.

## 304 **Conclusions**

305 In summary, this work demonstrates the utility of an anti-fogging formulation with two  
306 natural waxes that has good durability and optimal non-fouling properties. This solution represents  
307 a cost-effective, durable, non-toxic approach to prevent or reduce fogging of clear PPEs such as  
308 plastic masks and face shields from condensations of humidity arising from breathing and  
309 speaking.

## 310 **Conflicts of Interests**

311 The authors declare they have no relevant conflicts of interest with this work.

## 312 **Acknowledgements**

313 We thank the members of the Buffalo3DPPE for their time and effort during the pandemic namely,  
314 Kierra Bleyle, Preethi Singh, Jason Ciano, Savannah Tomaka, Jacob Graca, Hunter Rosa, Yianni  
315 Savidis, Danielle Detwiler, Omer Hillel, and Georgia Kyriacou. We also thank the Buffalo Enable  
316 (BE Mask) team for their valuable collaboration and technical assistance with 3D printing namely  
317 Aaron Gorsline, Albert Titus, James Whitlock, Peter Elkin, Jeremy Simon, Jon Schull, Ben Rubin,  
318 Kelly Cheadle, Pete Suffoletto, and Skip Meetze. We would like to thank Mr. Peter Bush, South  
319 Campus Instrument core for assisting with the SEM analysis and Weber Medical laser for  
320 providing their laser device.

## 321 **References**

- 322 1. Pak A, Adegboye OA, Adekunle AI, Rahman KM, McBryde ES, Eisen DP. Economic Consequences  
323 of the COVID-19 Outbreak: the Need for Epidemic Preparedness. *Front Public Health* 2020; 8:241.
- 324 2. Pirasteh-Anosheh H, Parnian A, Spasiano D, Race M, Ashraf M. Haloculture: A system to mitigate  
325 the negative impacts of pandemics on the environment, society and economy, emphasizing  
326 COVID-19. *Environ Res* 2021; 198:111228.
- 327 3. Goriuc A, Sandu D, Tatarciuc M, Luchian I. The Impact of the COVID-19 Pandemic on Dentistry and  
328 Dental Education: A Narrative Review. *Int J Environ Res Public Health* 2022; 19(5).
- 329 4. Kurian N, Gandhi S, Thomas AM. COVID-19 and multidisciplinary dentistry. *Br Dent J* 2021;  
330 231(9):534.
- 331 5. Lieberthal B, McCauley LK, Feldman CA, Fine DH. COVID-19 and Dentistry: Biological  
332 Considerations, Testing Strategies, Issues, and Regulations. *Compend Contin Educ Dent* 2021;  
333 42(6):290-296; quiz 297.
- 334 6. Artenstein AW. In Pursuit of PPE. *N Engl J Med* 2020; 382(18):e46.
- 335 7. Marcus K, Balasubramanian M, Short SD, Sohn W. Dental hesitancy: a qualitative study of  
336 culturally and linguistically diverse mothers. *BMC Public Health* 2022; 22(1):2199.
- 337 8. Muneer MU, Ismail F, Munir N, Shakoor A, Das G, Ahmed AR, Ahmed MA. Dental Anxiety and  
338 Influencing Factors in Adults. *Healthcare (Basel)* 2022; 10(12).
- 339 9. Nikolic M, Mitic A, Petrovic J, Dimitrijevic D, Popovic J, Barac R, Todorovic A. COVID-19: Another  
340 Cause of Dental Anxiety? *Med Sci Monit* 2022; 28:e936535.
- 341 10. Blais C, Fiset D, Roy C, Saumure Regimbald C, Gosselin F. Eye fixation patterns for categorizing  
342 static and dynamic facial expressions. *Emotion* 2017; 17(7):1107-1119.
- 343 11. Chodosh J, Weinstein BE, Blustein J. Face masks can be devastating for people with hearing loss.  
344 *BMJ* 2020; 370:m2683.
- 345 12. Chu JN, Collins JE, Chen TT, Chai PR, Dadabhoy F, Byrne JD, Wentworth A, DeAndrea-Lazarus IA,  
346 Moreland CJ, Wilson JAB, Booth A, Ghenand O, Hur C, Traverso G. Patient and Health Care Worker

- 347 Perceptions of Communication and Ability to Identify Emotion When Wearing Standard and  
348 Transparent Masks. *JAMA Netw Open* 2021; 4(11):e2135386.
- 349 13. Fleming JT, Maddox RK, Shinn-Cunningham BG. Spatial alignment between faces and voices  
350 improves selective attention to audio-visual speech. *J Acoust Soc Am* 2021; 150(4):3085.
- 351 14. MacLeod A, Summerfield Q. Quantifying the contribution of vision to speech perception in noise.  
352 *Br J Audiol* 1987; 21(2):131-141.
- 353 15. Schwartz JL, Berthommier F, Savariaux C. Seeing to hear better: evidence for early audio-visual  
354 interactions in speech identification. *Cognition* 2004; 93(2):B69-78.
- 355 16. Sonnichsen R, Llorach To G, Hochmuth S, Hohmann V, Radeloff A. How Face Masks Interfere With  
356 Speech Understanding of Normal-Hearing Individuals: Vision Makes the Difference. *Otol Neurotol*  
357 2022; 43(3):282-288.
- 358 17. Atcherson SR, Mendel LL, Baltimore WJ, Patro C, Lee S, Pousson M, Spann MJ. The Effect of  
359 Conventional and Transparent Surgical Masks on Speech Understanding in Individuals with and  
360 without Hearing Loss. *J Am Acad Audiol* 2017; 28(1):58-67.
- 361 18. Belhouideg S. Impact of 3D printed medical equipment on the management of the Covid19  
362 pandemic. *Int J Health Plann Manage* 2020; 35(5):1014-1022.
- 363 19. O'Connor S, Mathew S, Dave F, Tormey D, Parsons U, Gavin M, Nama PM, Moran R, Rooney M,  
364 McMorro R, Bartlett J, Pillai SC. COVID-19: Rapid prototyping and production of face shields via  
365 flat, laser-cut, and 3D-printed models. *Results Eng* 2022; 14:100452.
- 366 20. Rupesh Kumar J, Mayandi K, Joe Patrick Gnanaraj S, Chandrasekar K, Sethu Ramalingam P. A  
367 critical review of an additive manufacturing role in Covid-19 epidemic. *Mater Today Proc* 2022;  
368 68:1521-1527.
- 369 21. Vallatos A, Maguire JM, Pilavakis N, Cerniauskas G, Sturtivant A, Speakman AJ, Gourlay S, Inglis S,  
370 McCall G, Davie A, Boyd M, Tavares AAS, Doherty C, Roberts S, Aitken P, Mason M, Cummings S,  
371 Mullen A, Paterson G, Proudfoot M, Brady S, Kesterton S, Queen F, Fletcher S, Sherlock A, Dunn  
372 KE. Adaptive Manufacturing for Healthcare During the COVID-19 Emergency and Beyond. *Front*  
373 *Med Technol* 2021; 3:702526.
- 374 22. Kalkal A, Allawadhi P, Kumar P, Sehgal A, Verma A, Pawar K, Pradhan R, Paital B, Packirisamy G.  
375 Sensing and 3D printing technologies in personalized healthcare for the management of health  
376 crises including the COVID-19 outbreak. *Sens Int* 2022; 3:100180.
- 377 23. Arany PSaP. Dental Faceshields. 2020.
- 378 24. Wahab IF, Bushroa AR, Teck SW, Azmi TT, Ibrahim MZ, Lee JW. Fundamentals of antifogging  
379 strategies, coating techniques and properties of inorganic materials; a comprehensive review.  
380 *Journal of Materials Research and Technology* 2023; 23.
- 381 25. Laurén S. Contact angle measurements on superhydrophobic surfaces in practice. *Surface Science*  
382 *Blog: Biolin Scientific*; 2019.
- 383 26. Lv C, Yang C, Hao P, He F, Zheng Q. Sliding of water droplets on microstructured hydrophobic  
384 surfaces. *Langmuir* 2010; 26(11):8704-8708.
- 385 27. Razavi SMR OJ, Sett S, Feng L, Yan X, Hoque MJ, Liu Aihua, Haasch RT, Masoomi M, Bagheri R,  
386 Miljkovic N. Superhydrophobic Surfaces Made from Naturally Derived Hydrophobic Materials.  
387 *ACS Sustainable Chem Eng* 2017; 5(12):8.
- 388 28. Bormashenko E. Wetting of real solid surfaces: new glance on well-known problems. *Colloid and*  
389 *Polymer Science* 2013.
- 390 29. Li P. Submillimeter Papillae: Shape Control of Lotus Leaf Induced by Surface Submillimeter  
391 Texture. *Advanced Materials Interfaces* 2020.
- 392 30. Wang P QX, Shen J. Superhydrophobic Coatings with Edible Biowaxes for Reducing or Eliminating  
393 Liquid Residues of Foods and Drinks in Containers. *Bioresources* 2018.

- 394 31. Brill AK, Pickersgill R, Moghal M, Morrell MJ, Simonds AK. Mask pressure effects on the nasal  
395 bridge during short-term noninvasive ventilation. *ERJ Open Res* 2018; 4(2).
- 396 32. Dellweg D, Hochrainer D, Klauke M, Kerl J, Eiger G, Kohler D. Determinants of skin contact pressure  
397 formation during non-invasive ventilation. *J Biomech* 2010; 43(4):652-657.
- 398 33. Schettino GP, Tucci MR, Sousa R, Valente Barbas CS, Passos Amato MB, Carvalho CR. Mask  
399 mechanics and leak dynamics during noninvasive pressure support ventilation: a bench study.  
400 *Intensive Care Med* 2001; 27(12):1887-1891.
- 401 34. Epstein JB, Chow K, Mathias R. Dental procedure aerosols and COVID-19. *Lancet Infect Dis* 2021;  
402 21(4):e73.
- 403 35. Mick P, Murphy R. Aerosol-generating otolaryngology procedures and the need for enhanced PPE  
404 during the COVID-19 pandemic: a literature review. *J Otolaryngol Head Neck Surg* 2020; 49(1):29.
- 405 36. Wilson NM, Norton A, Young FP, Collins DW. Airborne transmission of severe acute respiratory  
406 syndrome coronavirus-2 to healthcare workers: a narrative review. *Anaesthesia* 2020; 75(8):1086-  
407 1095.
- 408 37. Kisielinski K, Giboni P, Prescher A, Klosterhalfen B, Graessel D, Funken S, Kempfski O, Hirsch O. Is a  
409 Mask That Covers the Mouth and Nose Free from Undesirable Side Effects in Everyday Use and  
410 Free of Potential Hazards? *Int J Environ Res Public Health* 2021; 18(8).
- 411 38. Rothe H, Fautz R, Gerber E, Neumann L, Rettinger K, Schuh W, Gronewold C. Special aspects of  
412 cosmetic spray safety evaluations: principles on inhalation risk assessment. *Toxicol Lett* 2011;  
413 205(2):97-104.
- 414 39. Tha EL, Canavez A, Schuck DC, Gagosian VSC, Lorencini M, Leme DM. Beyond dermal exposure:  
415 The respiratory tract as a target organ in hazard assessments of cosmetic ingredients. *Regul*  
416 *Toxicol Pharmacol* 2021; 124:104976.
- 417 40. Final Report on the Safety Assessment of Candelilla Wax, Carnauba Wax, Japan Wax, and  
418 Beeswax. *J Am Coll Toxicol* 1984; 3(3).
- 419 41. Arnesdotter E, Rogiers V, Vanhaecke T, Vinken M. An overview of current practices for regulatory  
420 risk assessment with lessons learnt from cosmetics in the European Union. *Crit Rev Toxicol* 2021;  
421 51(5):395-417.
- 422 42. Choksi NY, Truax J, Layton A, Matheson J, Mattie D, Varney T, Tao J, Yozzo K, McDougal AJ, Merrill  
423 J, Lowther D, Barroso J, Linke B, Casey W, Allen D. United States regulatory requirements for skin  
424 and eye irritation testing. *Cutan Ocul Toxicol* 2019; 38(2):141-155.
- 425 43. Filaire E, Nachat-Kappes R, Laporte C, Harmand MF, Simon M, Poinot C. Alternative in vitro  
426 models used in the main safety tests of cosmetic products and new challenges. *Int J Cosmet Sci*  
427 2022; 44(6):604-613.
- 428 44. Hardwick RN, Betts CJ, Whritenour J, Sura R, Thamsen M, Kaufman EH, Fabre K. Drug-induced skin  
429 toxicity: gaps in preclinical testing cascade as opportunities for complex in vitro models and  
430 assays. *Lab Chip* 2020; 20(2):199-214.
- 431 45. Nabarretti BH, Rigon RB, Burga-Sanchez J, Leonardi GR. A review of alternative methods to the  
432 use of animals in safety evaluation of cosmetics. *Einstein (Sao Paulo)* 2022; 20:eRB5578.
- 433 46. Pistollato F, Madia F, Corvi R, Munn S, Grignard E, Paini A, Worth A, Bal-Price A, Prieto P, Casati S,  
434 Berggren E, Bopp SK, Zuang V. Current EU regulatory requirements for the assessment of  
435 chemicals and cosmetic products: challenges and opportunities for introducing new approach  
436 methodologies. *Arch Toxicol* 2021; 95(6):1867-1897.
- 437 47. Riebeling C, Luch A, Tralau T. Skin toxicology and 3Rs-Current challenges for public health  
438 protection. *Exp Dermatol* 2018; 27(5):526-536.

439

## 440 **Figure Legends**

### 441 **Figure 1. Physical characterization of anti-fogging coating**

442 (A.) CAD of the contact angle apparatus for 3D printing (B.) CAD of the sliding angle module for  
443 3D printing (C.) 3D printed models of contact and sliding angle testing apparatus (D.) Image of  
444 the contact angle assessment showing droplet generation and analysis. Inset shows the digital  
445 analysis of contact angle  $\phi$  using NIH ImageJ (E.) Digital image analysis showing the sliding angle  
446 measurement using NIH ImageJ (F.) transmittance set-up using a diode laser and optical power  
447 meter with the sensor.

### 448 **Figure 2. Anti-fogging solution formulation and characterization**

449 (A.) Tabular outline of the formulation depicting ratios of carnauba and beeswax in acetone and  
450 methanol used to coat PETG plastic sheets (B. and C.) Contact angle assessment of Acetone and  
451 Methanol formulations at various concentrations (D and E) Sliding angle analysis of Acetone and  
452 Methanol formulations at various concentrations (F and G) Transmission of diode laser for  
453 transmittance assessment of Acetone and Methanol formulations at various concentrations. (I.)  
454 Digital image of an uncoated, Acetone and Methanol formulations applied to the PETG sheet. Data  
455 are shown as Mean and SD and representative of at least two independent studies. Statistical  
456 significance was determined using two-way analysis of variance (ANOVA) among different  
457 treatments using Bonferroni's multiple comparison test ( $n = 3$ ). Statistical significance is denoted  
458 as \*  $p < 0.05$ , \*\*  $p < 0.005$ , and \*\*\*  $p < 0.0005$ .

### 459 **Figure 3. Effects of Disinfection on anti-fogging coating integrity**

460 (A.) Contact angle assessment after various disinfection procedures (B.) Sliding angle analysis  
461 after various disinfection procedures (C.) transmittance after various disinfection procedures. Data  
462 are shown as Mean and SD and representative of at least two independent studies. Statistical  
463 significance was determined using two-way analysis of variance (ANOVA) among different  
464 treatments using Bonferroni's multiple comparison test ( $n = 3$ ). Statistical significance is denoted  
465 as \*  $p < 0.05$ , \*\*  $p < 0.005$ , \*\*\*  $p < 0.0005$ , and \*\*\*\*  $p < 0.00005$ .

466

467

468 **Figure 4. Durability testing of anti-fogging coating following contact testing**

469 (A.) CAD of contact testing apparatus used for wear testing analysis (B.) 3D printed model of the  
470 assembled contact testing apparatus (C.) Outline of the eminent forces determining the contact  
471 force on PETG surfaces. The contact angle (D.), sliding angle (E.), and transmittance (F.) analysis  
472 before and after contact testing (G.) Scanning electron microscopy images of the uncoated and  
473 coated surfaces before and after contact testing. Data are shown as Mean and SD and representative  
474 of at least two independent studies. Statistical significance was determined using the Students' T-  
475 test (n = 3). Statistical significance is denoted as \*  $p < 0.05$ .

476 **Figure 5. Clear face shields and masks**

477 A clear mask design with filter unit is shown (A.) The 3D printed clear face shields are shown to  
478 accommodate different dental operating loupes such as Eclipse (B.), Vision, Surgitel and  
479 Orascoptic (C.). Images are provided with consent from lab volunteers from the website  
480 [www.buffalo3dppe.com](http://www.buffalo3dppe.com).

# Figure 1

Figure 1. Physical characterization of anti-fogging coating

(**A.**) CAD of the contact angle apparatus for 3D printing (**B.**) CAD of the sliding angle module for 3D printing (**C.**) 3D printed models of contact and sliding angle testing apparatus (**D.**) Image of the contact angle assessment showing droplet generation and analysis. Inset shows the digital analysis of contact angle  $\phi$  using NIH ImageJ (**E.**) Digital image analysis showing the sliding angle measurement using NIH ImageJ (**F.**) transmittance set-up using a diode laser and optical power meter with the sensor.

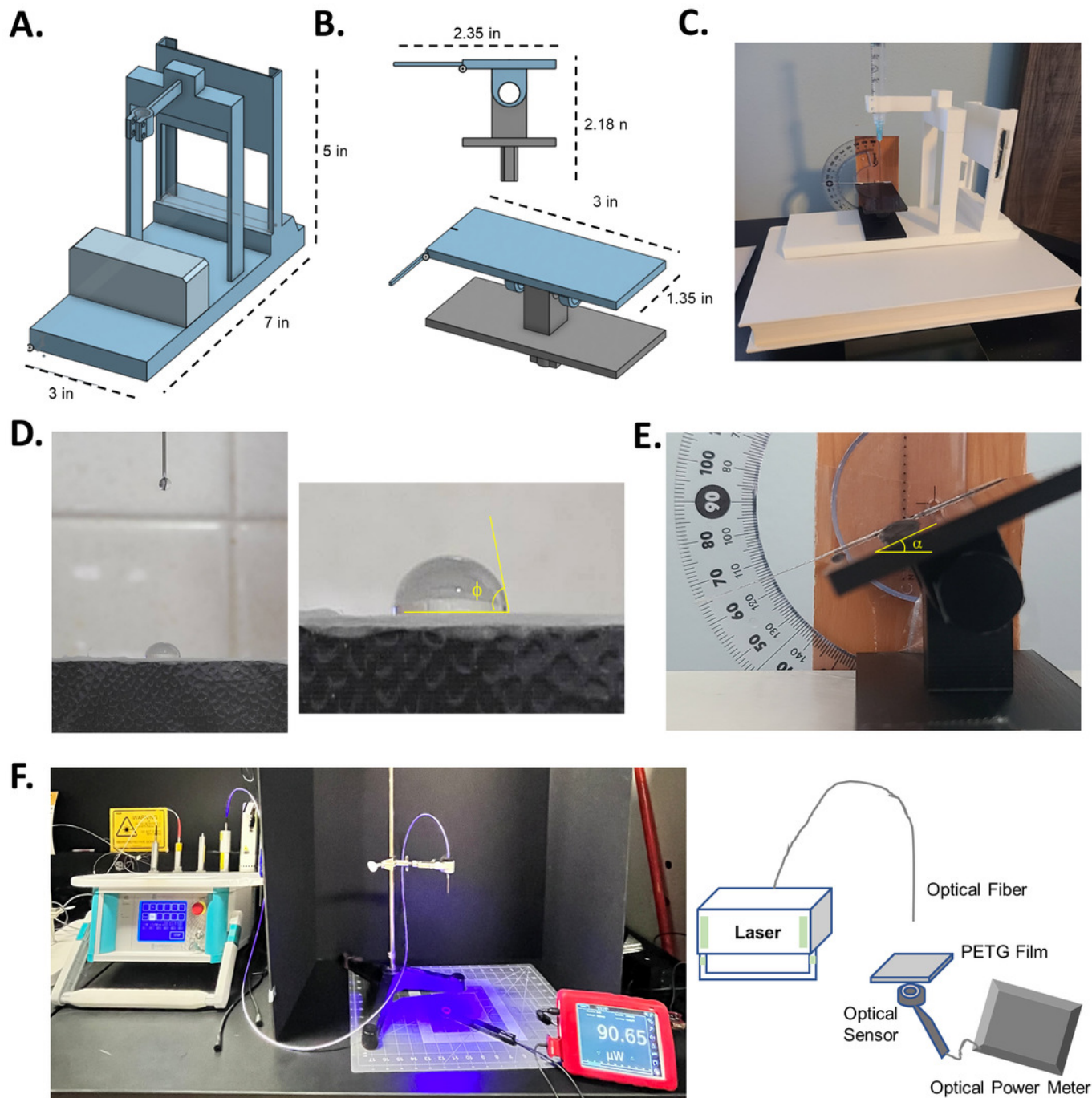


## Figure 2

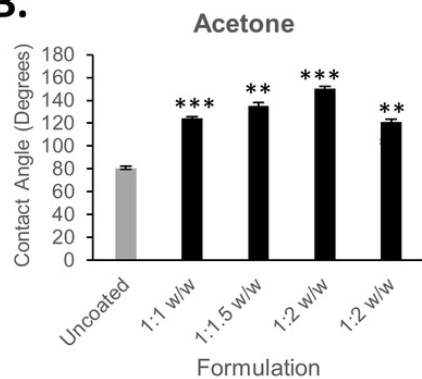
Figure 2. Anti-fogging solution formulation and characterization

**(A.)** Tabular outline of the formulation depicting ratios of carnauba and beeswax in acetone and methanol used to coat PETG plastic sheets **(B. and C.)** Contact angle assessment of Acetone and Methanol formulations at various concentrations **(D and E)** Sliding angle analysis of Acetone and Methanol formulations at various concentrations **(F and G)** Transmission of diode laser for transmittance assessment of Acetone and Methanol formulations at various concentrations. **(I.)** Digital image of an uncoated, Acetone and Methanol formulations applied to the PETG sheet. Data are shown as Mean and SD and representative of at least two independent studies. Statistical significance was determined using two-way analysis of variance (ANOVA) among different treatments using Bonferroni's multiple comparison test ( $n = 3$ ). Statistical significance is denoted as \*  $p < 0.05$ , \*\*  $p < 0.005$ , and \*\*\*  $p < 0.0005$ .

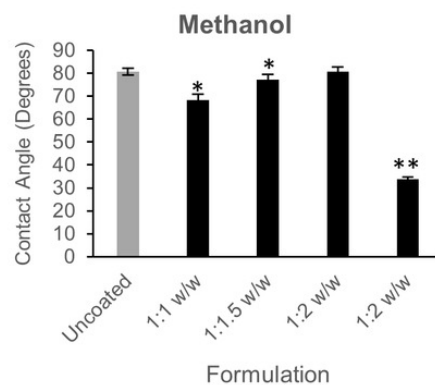
A.

Ratio	Carnauba (g)	Beeswax (g)	Acetone/Methanol (ml)
1:1	0.4375	0.4375	25
1:1.5	0.35	0.525	25
1:2	0.33	0.67	25
1:2 (HC)	0.417	0.833	25

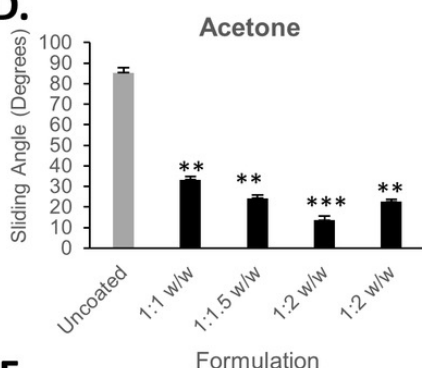
B.



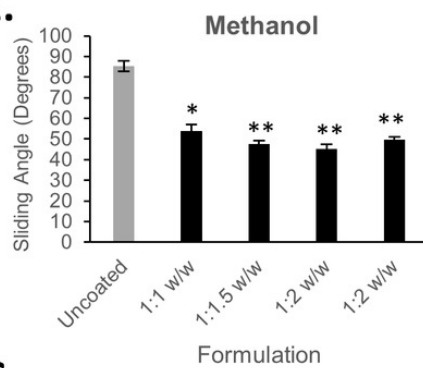
C.



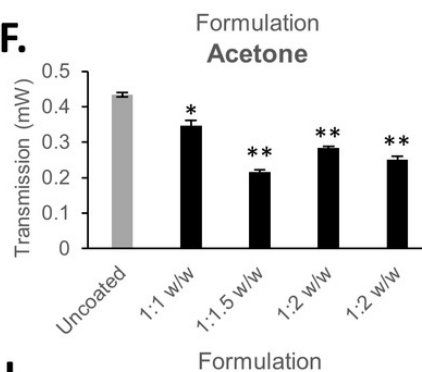
D.



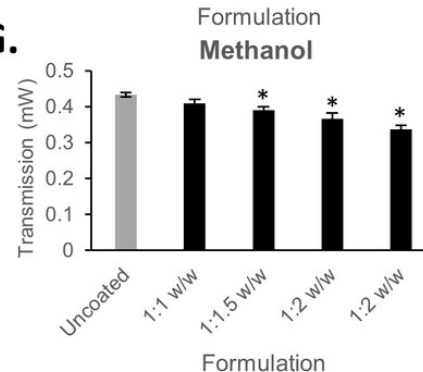
E.



F.



G.



I.



## Figure 3

Figure 3. Effects of Disinfection on anti-fogging coating integrity

**(A.)** Contact angle assessment after various disinfection procedures **(B.)** Sliding angle analysis after various disinfection procedures **(C.)** transmittance after various disinfection procedures. Data are shown as Mean and SD and representative of at least two independent studies. Statistical significance was determined using two-way analysis of variance (ANOVA) among different treatments using Bonferroni's multiple comparison test ( $n = 3$ ). Statistical significance is denoted as \*  $p < 0.05$ , \*\*  $p < 0.005$ , \*\*\*  $p < 0.0005$ , and \*\*\*\*  $p < 0.00005$ .

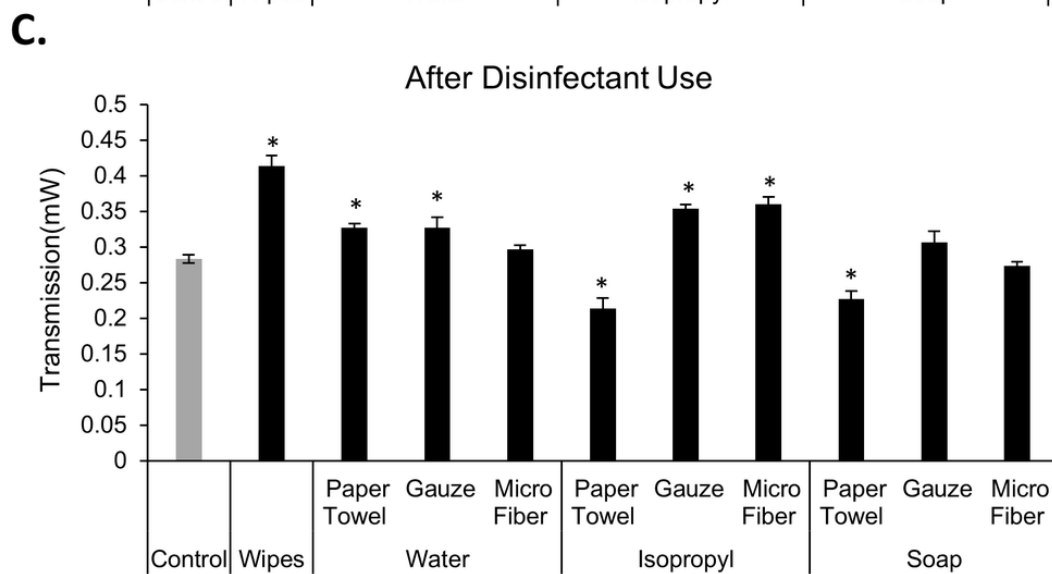
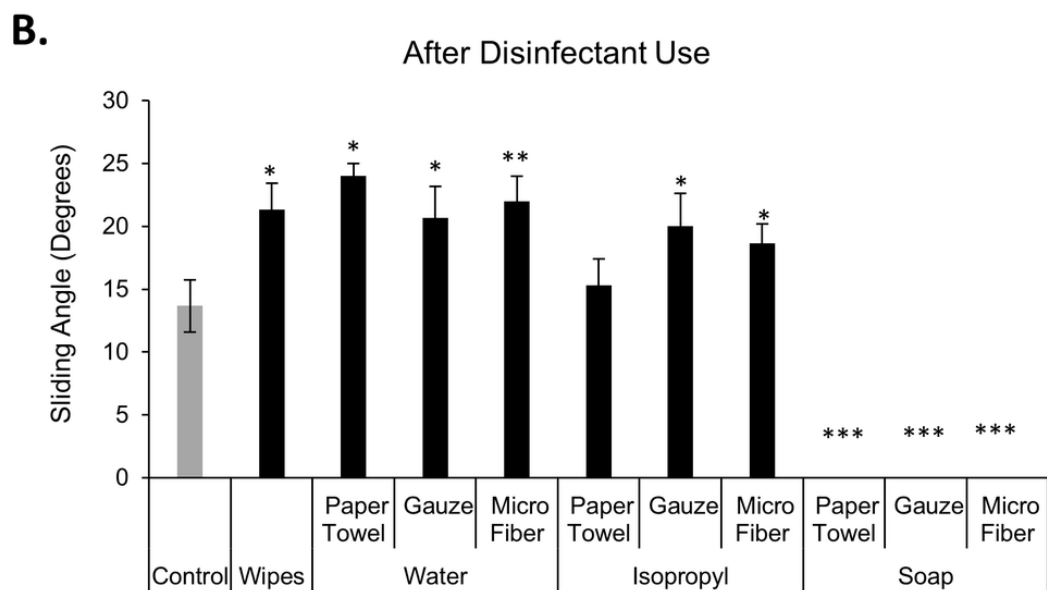
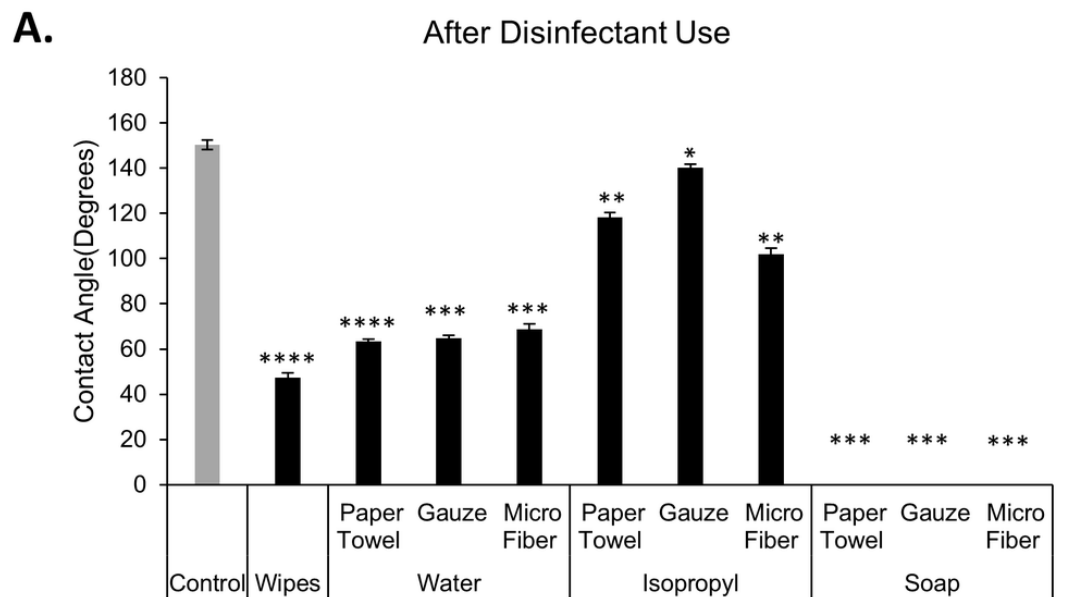


## Figure 4

Figure 4. Durability testing of anti-fogging coating following contact testing

(**A.**) CAD of contact testing apparatus used for wear testing analysis (**B.**) 3D printed model of the assembled contact testing apparatus (**C.**) Outline of the eminent forces determining the contact force on PETG surfaces. The contact angle (**D.**), sliding angle (**E.**), and transmittance (**F.**) analysis before and after contact testing (**G.**) Scanning electron microscopy images of the uncoated and coated surfaces before and after contact testing. Data are shown as Mean and SD and representative of at least two independent studies. Statistical significance was determined using the Students' T-test ( $n = 3$ ). Statistical significance is denoted as \*  $p < 0.05$ .

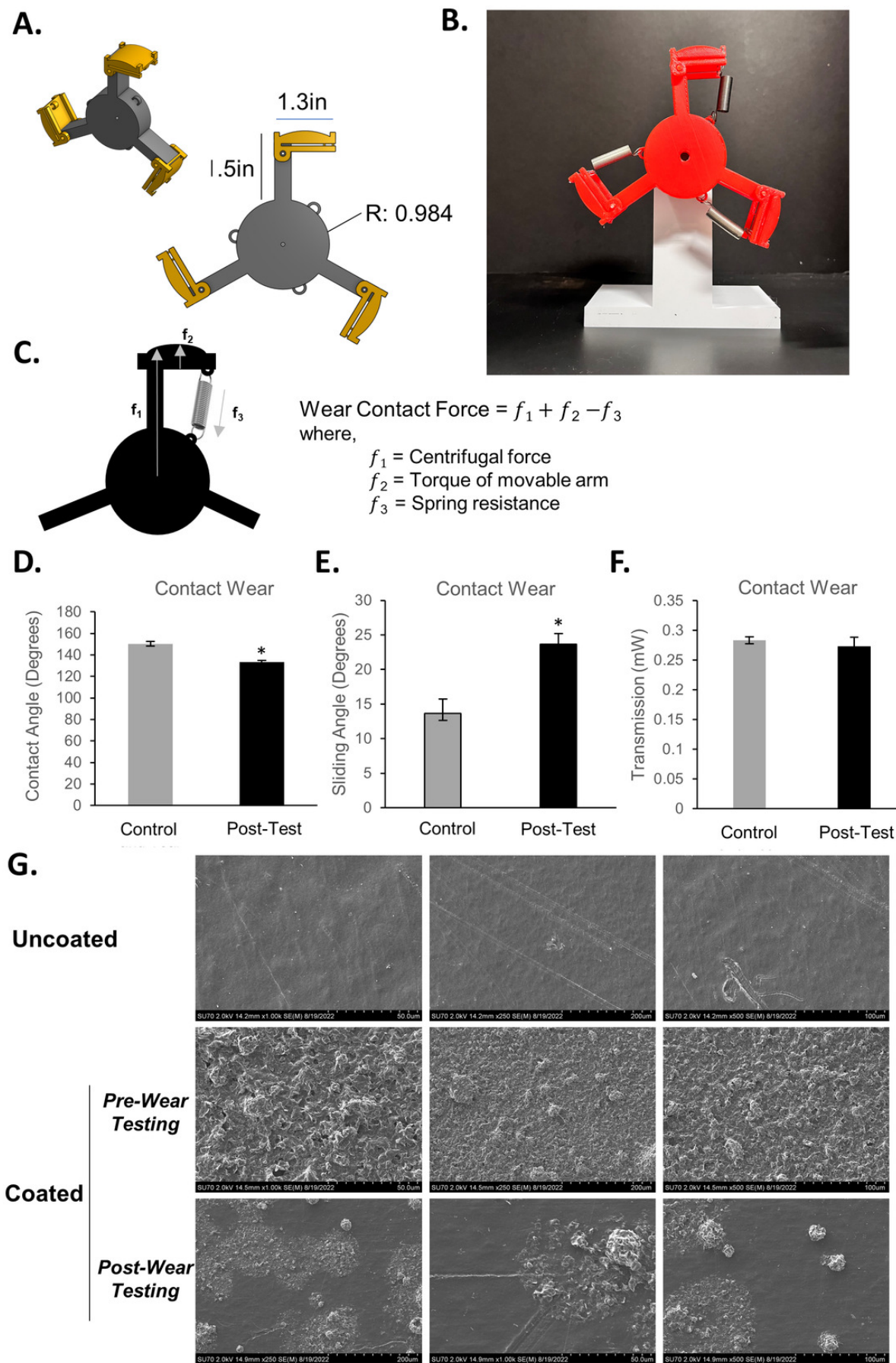


## Figure 5

Figure 5. Clear face shields and masks

A clear mask design with filter unit in medium (**A.**) and large (**B.**) sizes. The 3D printed clear face shields are shown to accommodate different dental operating loupes such as Eclipse (**C.**), Vision, Surgitel and Orascoptic (**D.**). Images are provided with consent from lab volunteers from the website [www.buffalo3dppe.com](http://www.buffalo3dppe.com) .

**A.****B.****C.**